Evaluating the Energy Performance
of Ballasted Roof Systems

Andre O. Desjarlais, Thomas W. Petrie and Jerald A. Atchley
Building Envelopes Program, Oak Ridge National Laboratory,
Richard Gillenwater, Carlisle SynTec, Inc.,
and David Roodvoets, SPRI

Evaluating the Energy Performance of Ballasted Roof Systems

Andre O. Desjarlais, Thomas W. Petrie, Jerald A. Atchley, ORNL,
Richard Gillenwater, Carlisle SynTec, Inc.,
and David Roodvoets, SPRI

Abstract

It is well known that the mass of a ballasted roof can reduce peak roof temperatures and delay the heat flow into a building. Although ballasted roofs perform these "cool" functions, they do not meet the traditional requirement of high solar reflectance. This is one of the criteria set out by the Environmental Protection Agency (EPA) and other organizations in order for a roof to be "cool."

To address whether ballasted roofing systems offer energy efficiency benefits similar to cool roofs, a project to perform side-by-side experiments was initiated. Different loadings of stone-ballasted roofs and an uncoated paver-ballasted roof were compared to roofs under exposed black and white membranes. The six test sections were constructed and installed on a test building at the Oak Ridge National Laboratory and monitored for energy performance for thirty-six months. One year into the project, systems with two loadings of pavers coated with a white coating were added. They were monitored along with the other six systems for the rest of the thirty-six month period.

Data collection included continuous monitoring of temperatures, heat flows and weather conditions as well as periodic verification of the solar reflectance of each surface. These data answer what impact a ballasted roof has on heat flow into a building and on roof surface temperature. Furthermore, comparisons between the ballasted and unballasted membranes allow for an assessment of whether ballasted systems perform as well as white membranes and are deserving of "cool roof" status within the codes. The cooling loads show that the heaviest and medium stone-ballasted and the uncoated paver-ballasted systems perform as well as the white system. The coated paver systems outperform it.

This report also describes the modeling of the energy performance of all systems with the Simplified Transient Analysis of Roofs (STAR) program. STAR does well for light weight roofs with exposed membranes. Reasonable values of effective specific heat and thermal conductivity were sought for the ballasted systems in order to get good agreement between the predicted and measured membrane temperatures and insulation heat fluxes on several clear and sunny days during the project. These properties were used to predict annual cooling and heating loads for comparison to the measured loads for all three years of the project. Modeling of ballasted roofs was desired so that the experimental results from East Tennessee could be generalized to more typical R-values than the low R-values selected to maximize experimental responses and to other climates. The modeling verified that the measured trends persisted with more typical roof R-values and in locations with more severe cooling requirements than during the tests.

Introduction

Ballasted systems entered the roofing market in the early 1970's. The stone used with these systems is different from the traditional ¼-in. chip or smaller stone used with built-up and modified bitumen roofing. With these systems the small stones are partially imbedded into the topcoat of asphalt to protect the asphalt from the harmful ultraviolet rays of the sun. The same strategy applies to coal-tar-based systems. The stone used as ballast for single ply systems is large in size, #4 (0.75 to 1.5 in. diameter) and larger stone. Ballast comes in other configurations such as concrete or rubber pavers. Ballast is applied in loadings from the minimum of 10 lb/ft^2 to over 24 lb/ft^2.

With the loose-laid ballasted roof system, the contractor places all the components of the roof system, including the thermal barrier and insulation, unattached on the roof deck. The membrane is also loose-laid except for attachment around the perimeter of the building and at roof penetrations. The ballast is then placed on top of the membrane weighting down all the components to hold them in place. This technique eliminates use of fasteners to hold the roofing components in place. This in turn minimizes thermal bridging and other problems from use of many fasteners to secure the roof against wind uplift.

Ballast is also used with the inverted - protected roof system for which the roof system is built "upside down." A protective course may be placed over the deck. The membrane is then laid down, followed by the insulation, a filter fabric and the ballast. The ballast often used in this application is pavers because the typical situation has pedestrian traffic on the roof. Plaza decks and roof top terraces are a few examples. The paver offers a trafficable surface with the insulation acting as both a thermal protection layer and a shock absorber for the waterproofing system below it. Another form of ballast is mixed soil media and plants to form a roof garden with unique aesthetic appeal and performance characteristics such as storm water management.

Early proponents of ballasted roofing systems focused mainly on how to design them to resist the destructive powers of the wind. This led to a number of wind performance issues toward the end of the 70's and into the early 80's. The wind issues energized the industry to find ways to design a ballasted system for specific wind zones. Extensive wind tunnel work was conducted with thorough verification of the modeling through field observations. All this work led to the ANSI/SPRI RP-4 national standard entitled "Wind Design Standard for Ballasted Single-Ply Roofing Systems" (ANSI/SPRI, 2001). This standard outlines design procedures for ballasted systems that address wind loads on various building configurations in locations across the country. This standard has proven its merits: ballasted systems survived major storm events including the hurricane seasons of 2004 and 2005.

In recent years, roofing membranes offering highly reflective surfaces have become the new rage of the industry, government and code agencies. These membranes are used in fully adhered and mechanically fastened roof systems to take advantage of the reflective property of the membrane. With reflective systems offering aesthetically pleasing roofs that assist in saving energy for the building owner, ballasted systems now seem a little old fashioned and out of step with the times. Is this truly the case or are there attributes of ballasted systems that have not been identified?

An experimental study was initiated to quantify the energy savings of ballasted roofing systems and to compare their energy performance to that of "cool roof" membranes. The experimental design was initially structured to evaluate how the mass of three different stone ballast loadings and one uncoated paver ballast affected heat flux into the building and the buildup of the membrane surface temperature in comparison to the controls. In this project, both a black and a white single-ply membrane served as

controls. Two additional paver ballasts, coated with a highly reflecting white coating, were deployed a year into the project when more space became available on the test building. Experimental work included the initial and subsequent occasional measure of solar reflectance and estimate of the infrared emittance of the test samples, weekly organization of the temperature and heat flux data, and comparison of the energy performance of the systems to that of the white and black controls.

This work builds on the earlier work completed and published in "The Field Performance of High-Reflectance Single-Ply Membranes Exposed to Three Years of Weathering in Various U.S. Climates" (Miller *et al*., 2002). That report was prepared by the Oak Ridge National Laboratory (ORNL) for The Single-Ply Roofing Industry (SPRI). The study investigated the solar reflectance and energy performance of single-ply membranes when exposed to the outdoor environment.

Three years of experimental data have been compiled for the current project. To date, two research papers have been written and presented from the results. Gillenwater *et al.* (2005) gave details on the construction and instrumentation of the systems. They presented and discussed the measured membrane temperatures and insulation heat fluxes during the first year of monitoring before deployment of the reflective pavers. Desjarlais *et al.* (2006) reviewed the behavior of the membrane temperatures and insulation heat fluxes through two years of monitoring. A third paper has been accepted to summarize results from the measurements for all three years and from the modeling effort.

Modeling the stone for its energy performance was one of the goals of this project from the outset. The uncoated and coated paver ballasts were included to aid in developing the model. If successful, a model could eventually allow ballast to be entered as a roof component in the DOE Cool Roof Calculator (Petrie *et al.* 2001, Petrie *et al.* 2004). Such a generalization of the experimental results would permit the annual heating and cooling loads to be estimated for specific ballast configurations on roofs with various insulation levels located in different regions of the country.

This report describes the experimental work and the effort to model the energy performance of the ballasted systems for all three years of the project. The thermal and physical properties of the various configurations are used as input to the one-dimensional transient heat conduction equation that is programmed in finite difference form in Simplified Transient Analysis of Roofs (STAR) (Wilkes, 1989). STAR is the modeling tool used in the development of the DOE Cool Roof Calculator. The purpose of the modeling is to achieve good agreement between two predicted and measured quantities for several clear days during the project. One is the temperature of the control membranes and of the black membranes under the ballasts. The other is the heat flux at the interface between the two pieces of fiberboard that comprise the insulation in each system. The properties to achieve this agreement are then used to predict cooling and heating loads for comparison to loads from the measurements.

Experimental Facilities

The Roof Thermal Research Apparatus (RTRA) at the Oak Ridge National Laboratory near Knoxville, TN was constructed in the late 1980's for documenting the effects of long-term exposure of small, low-slope roof test sections to the East Tennessee climate. The RTRA has four 4 ft by 8 ft openings in its roof to house instrumented low-slope roof test sections. Each test section may be divided into multiple areas. The original use of the RTRA showed in-service aging effects with CFC and alternative blowing agents for polyisocyanurate foam insulation boards in roofs covered by black and white membranes. In the late 1990's, the RTRA was used to document the energy performance of uncoated low-slope roofs side-by-side with ones coated with reflective coatings. Each test section was divided into 2 ft by 2 ft

areas with as many as eight different surfaces on a test section. For the ballast project, each test section was divided into two 4 ft by 4 ft areas. One contained the stone-ballasted systems for the 10 lb/ft^2 and 17 lb/ft^2 tests. The second contained the 24 lb/ft^2 tests, both stone and uncoated paver. The third contained control systems, one with an exposed black membrane and the other with an exposed white membrane. The fourth, deployed one year into the project, had two loadings of pavers, 21 and 16 lb/ft², coated with highly reflective white Decothane, a high solids elastomeric single pack polyurethane coating.

Figure 1 is a photograph of the RTRA that shows the entire building including a weather station. A dedicated data acquisition system is housed inside the RTRA. It acquires the outside temperature and relative humidity and the wind speed and direction 10 ft above the roof of the RTRA. The total horizontal solar insolation and the total horizontal infrared radiation are measured at the top of the railing in Figure 1. There are also many dedicated input channels for thermocouples and for millivolt signals, such as those produced by heat flux transducers. Jack panels, hardwired to the data acquisition system, are conveniently located under the test sections on the inside of the RTRA walls to make for short lead wires from the test sections to the jack panels. Data are acquired under control of a database that is specific to each experiment. The database instructs the data acquisition program as to what data to acquire and how often. Most channels are polled every minute. Data are stored in a compressed historical record. For ongoing experiments, averages every 15 minutes of all variables are written weekly to a spreadsheet. Special reports can be generated for further detail on time dependency down to the frequency in the historical record.

Figure 1. Roof Thermal Research Apparatus with weather station.

Test Sections

Figure 2 is a photograph taken on top of the RTRA that shows the four test sections used for the ballast project after deployment of the coated pavers one year into the project. The coated pavers and controls are in the foreground and the other ballasted systems are in the background. In between is an uninstrumented area that can be used for unmonitored exposure of materials. Figure 5, discussed later, shows a closeup of a stone-ballasted test section.

Figure 2. Test sections configured for the ballast tests.

To begin construction of the ballasted systems, uncoated pavers 2 in. thick and 2 ft square were weighed on a scale to determine their weight per unit area. Three of the four pavers required for a 4 ft square test section were sawed in half in order not to have any seams at the center of the uncoated paver test section. A whole paver occupies the center and halves complete it. The required weight of stone in the test area to achieve the same loading as the uncoated pavers comprised the heaviest stone. The lightest stone ballast loading was set at 10 lb/ft^2, which is the minimum allowed for a ballast system, and it did provide 100 percent coverage of the membrane. The loading of the third stone ballast was set at the average of the heaviest and lightest loadings. Buckets were used to carry the #4 stone from the scale to the roof of the RTRA where it was distributed inside frames to confine the ballast to its assigned area. Exactly enough stone was used to achieve 10.0, 16.8, and 23.5 lb/ft^2 loadings.

Separate determinations were made of the weight of stone to exactly fill a bucket and the volume of the bucket. This yielded a density of 92.4 lb/ft^3 for the stone. The space around the stones was also determined by the weight of water to displace it. This yielded a porosity of 40% for the stone. Dividing each loading by the density of the stone yielded average thicknesses of 1.3, 2.2 and 3.1 in., respectively, for the three stone-ballasted systems. Due to the nature of the stone, the thicknesses varied over the area of each stone test section.

The instrumentation for each test section is shown in Figure 3. The metal decks are exposed to the conditions inside the RTRA, which is maintained year round between 70°F and 80°F by an electric resistance heater and a small through-the-wall air conditioner. The membranes, in the case of the unballasted controls, or the top surfaces of the ballast, for the other test sections, are exposed to climatic conditions. Thermocouples on the decks and at the top of the test sections monitor the direct response to the imposed conditions. Additional thermocouples are at the internal interfaces. Wood fiberboard insulation with 1.5 in. thickness is used to maximize sensitivity to differences among the test sections.

At the interface between the 1 in. thick and 0.5 in. thick pieces of insulation, a heat flux transducer (HFT) is embedded in the top of the thicker insulation board. Each HFT was calibrated in the same configuration. Thermocouples are deployed at the level of each HFT, 6 in. and 12 in. from its center to
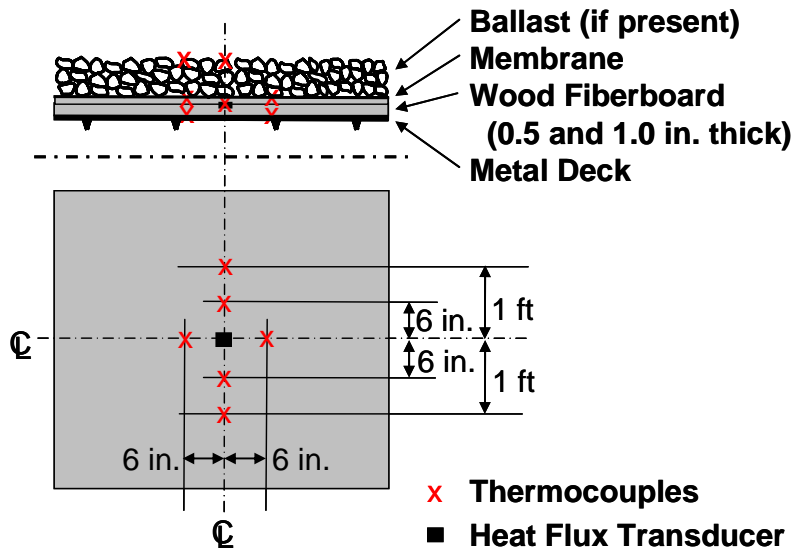
Figure 3. Thermocouple and heat flux transducer placement relative to the center of each test section.

monitor if there is any significant heat flow in the horizontal direction. Thermocouples at the other levels are 6 in. from the center of the test section.

The irregular upper surface of the stone-ballasted test sections presents a special challenge for monitoring surface temperature. Figure 4 shows the scheme that was adopted. Aluminum wire is strung across the middle of the frame from side to side in both directions. Thermocouples are attached to the wires with plastic wire ties. The lead wire between each measuring junction and its nearest wire tie is bent to hold the measuring junction against a stone and glued to the top of each test section. At the top of the paver-ballasted test sections a shallow hole was drilled into the top of the central paver, about 6 in. from its center. A thermocouple was epoxied in place so its measuring junction touched the bottom
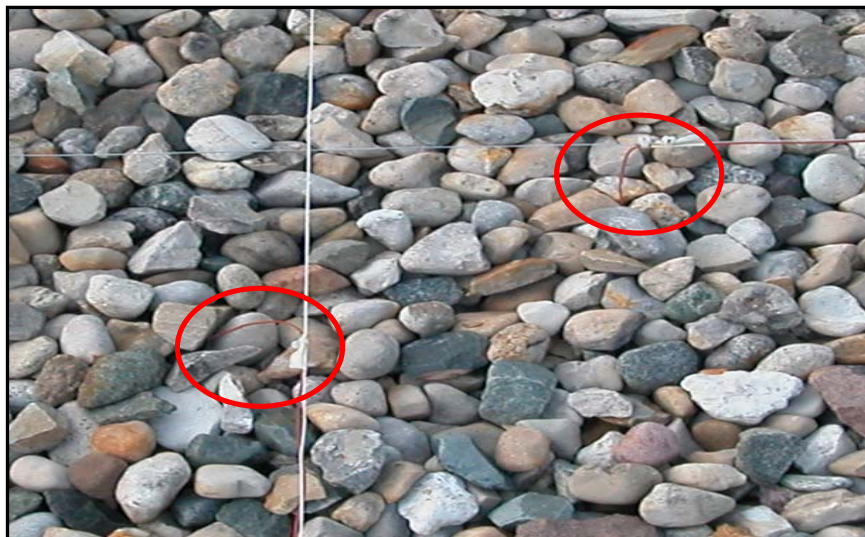

Figure 4. Thermocouple measuring junctions placed against pieces of stone at the top of the stone-ballasted test sections.

of the hole.

A property of primary interest for understanding the energy performance of roofs is the solar reflectance of the roof surface. It was measured for the surfaces of the test sections with two different techniques. For the smooth surfaced controls and the relatively smooth surfaced pavers, a Devices & Services solar spectrum reflectometer was taken onto the RTRA and used according to ASTM C 1549-04, Standard Test Method for Determination of Solar Reflectance Near Ambient Temperature Using a Portable Solar Reflectometer (ASTM, 2004 and Petrie, 2000). Table 1 summarizes the variation of solar reflectance for the smooth surfaces over the course of the project. Measurements were made near the beginning and end of each period and were interpolated to the middle of the seasons listed. The summers are six month intervals starting in late April and ending in late October. The winters start in late October and end in late April.

Table 1.
Variation of solar reflectance for the smooth surfaces in the project

Solar reflectance, %	Summer 2004	Winter 2004	Summer 2005	Winter 2005	Summer 2006	Winter 2006
White TPO membrane	70.5	63.7	61.8	60.4	60.7	60.5
Black EPDM membrane	8.0	8.9	9.4	9.1	9.0	8.8
Uncoated paver	54.0	52.0	49.4	49.3	48.9	47.2
21 lb/ft² coated paver	--	--	72.8	71.4	70.9	71.5
16 lb/ft² coated paver	--	--	74.1	75.2	76.1	75.6

The white TPO and uncoated paver showed effects of weathering. The TPO was fully weathered in less than two years. Its solar reflectance then stayed relatively constant for the rest of the project. The paver showed a similar pattern with smaller decreases but an additional decrease in Winter 2006. The black EPDM did not show much increase in solar reflectance as it weathered even though graying is a common phenomenon for initially black surfaces. The coating on the pavers proved to be resistant to weathering effects during the two years of exposure. No effort was made to clean any of the surfaces in order to restore solar reflectance lost during the project due to weathering.

For the stone-ballasted test sections, a custom-made roof surface albedometer was taken onto the RTRA and used with guidance from ASTM E 1918-97, Standard Test Method for Measuring Solar Reflectance of Horizontal and Low-Sloped Surfaces in the Field (ASTM, 1997). From data obtained at the beginning of each year of the project, solar reflectance of the stone did not change. The average for all the stone-ballasted test sections was 20% with two standard deviations (95% confidence) about it of ±1.4%.

An albedometer measures the solar reflectance of a surface as the ratio of the output of a solar spectrum pyranometer when inverted (facing downward toward the surface) and facing upward during an interval of constant solar irradiance. The area of the stone-ballasted test sections is only 4 ft by 4 ft, not the 13 ft by 13 ft recommended in E 1918 for use of the instrument. In order to minimize the effect of shadows from the assembly on the test section during use of the albedometer, a standard 20 in. height of the sensor above test sections is specified.

Because of the relatively small size of the ballasted test sections, the standard height was relaxed to 4 in. Lack of effect of this height was verified by extensive trials. A special support stand achieved the height of 4 in. above the surfaces. The stand held the pyranometer and its support arm steady and level during

the measurements. Figure 5 is a photograph of the albedometer in place over the surface of one stone-ballasted test section.

The inset shows the designer of the custom-made albedometer, the late Ross Robertson of Firestone Building Products, adjusting it to the 4 in. height. Ross brought the apparatus to Oak Ridge at the start of each year of the project to assist with the measurements. He also oversaw the fabrication and deployment of the coated pavers. His sudden and unexpected death near the end of the project meant he could not see its final results and lend his insights to conclusions from it. He was eager to contribute however he could to this project and set the standard for a contributing partner in user agreements.

A property of secondary interest for the energy performance of roofs is the infrared emittance of the roof surface. It is difficult to measure for thermally massive systems, especially the irregular surfaces of the stone-ballasted systems. In general, non-metallic surfaces have infrared emittance near 0.9. This value is

Figure 5. Use of a custom-made albedometer to measure the solar reflectance of the 4 ft square stone-ballasted test sections. Inset shows adjustment of the height of the albedometer to 4 in. above the stone surface.

assumed to apply to all the test sections in the ballast study and has been verified often in the SPRI study for single-ply white and black membranes (Miller, *et al.*, 2002).

Experimental Results

The ballast study went live on March 12, 2004 with the start of data collection, which continued uninterrupted through April 22, 2007. Figure 6 depicts the membrane temperature and heat fluxes through the six roof assemblies for a twenty-four hour period on 5 April 2004. These data start at
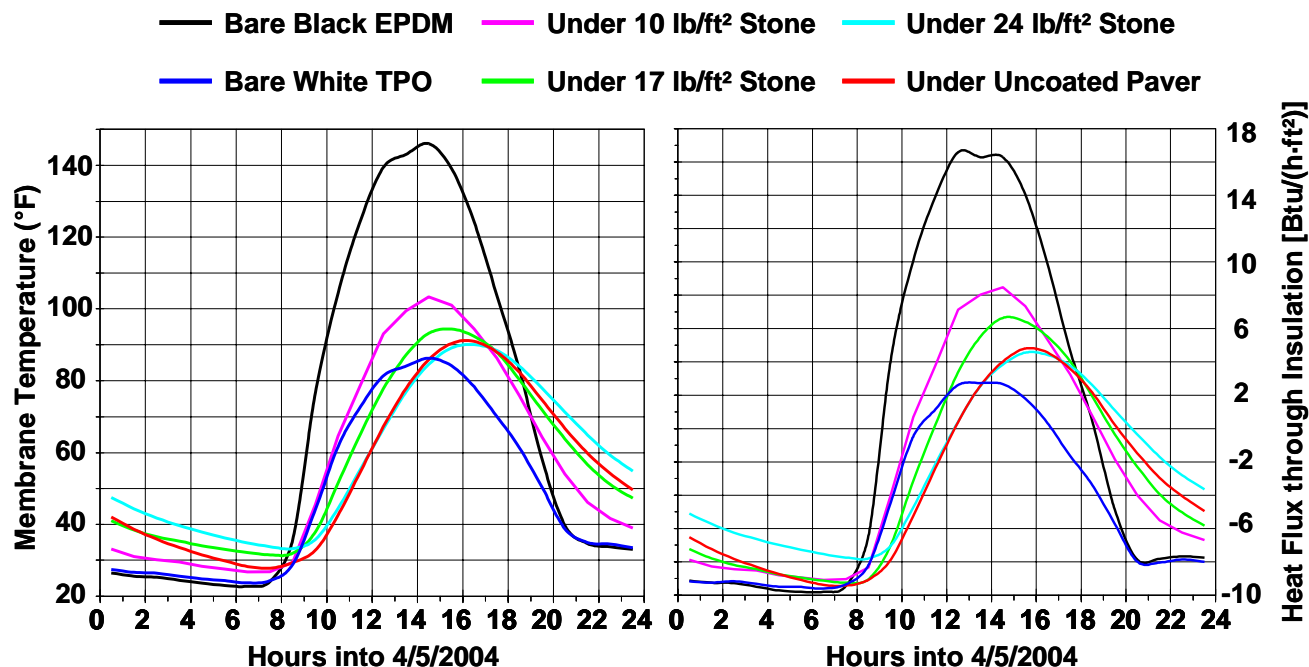

Figure 6. Membrane temperatures and roof heat fluxes one month into experimental program.

midnight (Hour 0) and were compiled approximately one month after the experiments started but just before the Summer 2004 period in Table 1. Hourly averages were formed at the end of each hour and are plotted at the midpoint of the hour.

In Figure 6, the black membrane shows the maximum temperature, peaking at approximately 146ºF. The white membrane shows the lowest peak temperature of 86ºF. Between the two extremes are the temperatures for the membranes covered by the three stone ballasts and the uncoated paver. The three stone-ballasted systems have peak membrane temperatures of 103°F, 95°F and 90ºF, respectively. The membrane under the uncoated paver has approximately the same peak temperature as the stone system having the same areal density. The ballasted systems show a delay in the peak temperature that ranges from 30 minutes to two hours. The delay increases as the areal density increases. The thermal inertia of the stone and paver ballasts can also be seen in the nighttime behavior. The energy storage in the massive systems keeps them warmer throughout the nighttime hours.

The heat flux data in Fig. 6 corroborate the temperature data. Peak heat fluxes are arranged in the identical order as the peak temperatures. After one month of performance, the white membrane has the lowest peak temperature and heat flux. This suggests that it is outperforming the other roof systems in terms of reducing cooling energy loads and peak demand.

Figures 7 through 12 depict the membrane temperature and heat fluxes for the six then eight roof assemblies for a twenty-four hour period on 4 October 2004, 21 March 2005, 5 October 2005, 23 May 2006, 4 October 2006 and 22 April 2007, respectively. These data start at midnight (Hour 0) and were compiled for clear days in fall and spring throughout the project. After seven months in service, as

shown in Fig. 7, the black membrane continues to have the warmest membrane reaching a peak temperature of 150ºF. Unlike in the initial results, the white membrane is no longer the coolest surface. After only seven months of service the 24 lb/ft^2 stone loading as well as the uncoated paver now have peak membrane temperatures that are lower than that of the white system. The 17 lb/ft^2 ballast loading
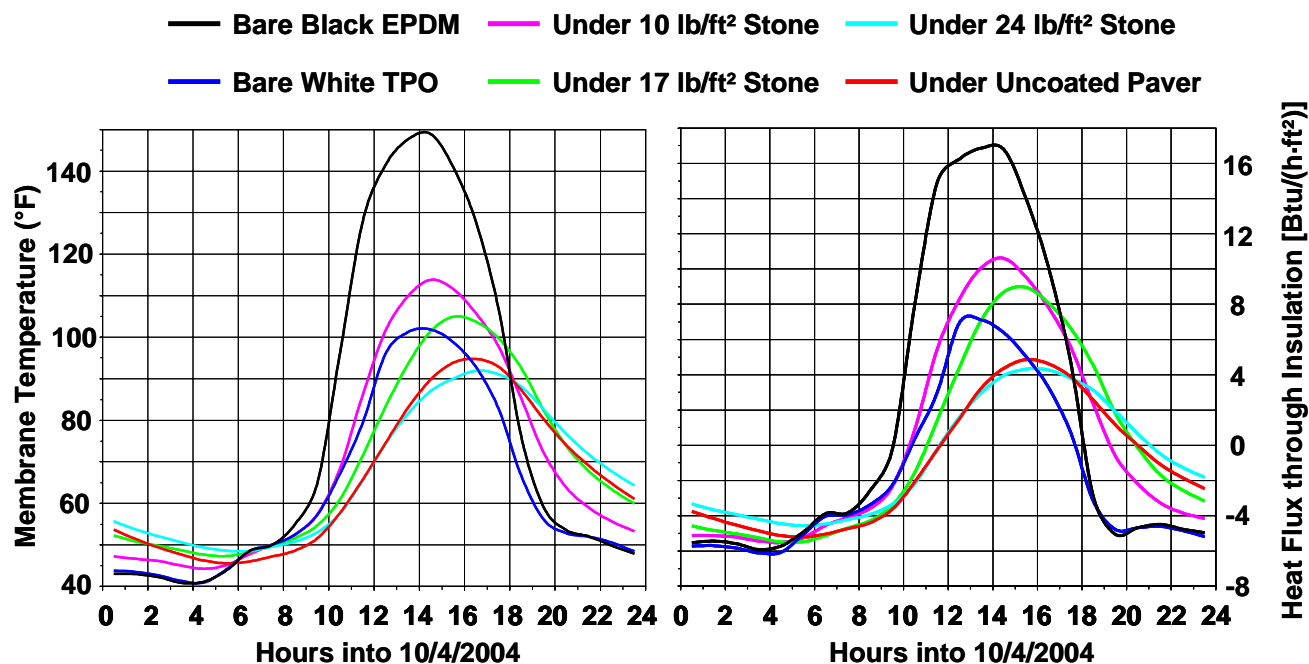

Figure 7. Membrane temperatures and roof heat fluxes seven months into experimental program.

has a peak membrane temperature almost equal to that of the white membrane. Similar to what was seen in Fig. 6, the ballast loadings delay the peak membrane temperatures and heat fluxes. Delays from one to three hours are measured and the delays increase with increasing levels of mass.

It is interesting to note that the heaviest stone-ballasted system and the uncoated paver have identical areal densities but substantially different solar reflectances. The stone and uncoated paver have solar reflectances of 0.20 and 0.54, respectively, after seven months. Their identical performance strongly suggests that the controlling parameter is the mass and not the solar reflectance.

The heat fluxes have the same trends as the temperatures. The 24 lb/ft^2 stone-ballast loading as well as the uncoated paver now have peak heat fluxes lower than the white system, 4.5 vs. 7.0 Btu/(h·ft^2). The black system has the highest peak heat flux, 17.0 Btu/(h·ft^2) on the day shown.

After twelve months of exposure in East Tennessee (see Fig. 8), the black membrane continues to be the warmest, reaching a peak temperature of 146ºF. Like after seven months, the 24 lb/ft^2 stone-ballasted system as well as the uncoated paver have peak membrane temperatures that are 9ºF lower than the peak for the white membrane. In addition, the 17 lb/ft^2 ballast loading has a slightly lower peak temperature than the white membrane (approximately 1ºF cooler). After twelve months, the black membrane continues to exhibit the highest peak heat flux, 16.8 Btu/(h·ft^2) on this day. The 24 lb/ft^2 stone-ballasted system as well as the uncoated paver have peak heat fluxes that are 4.2 and 4.6 Btu/(h·ft^2). These peaks are lower than the 7.3 and 9.0 Btu/(h·ft^2) peaks for the white and 17 lb/ft^2 stone systems, respectively.
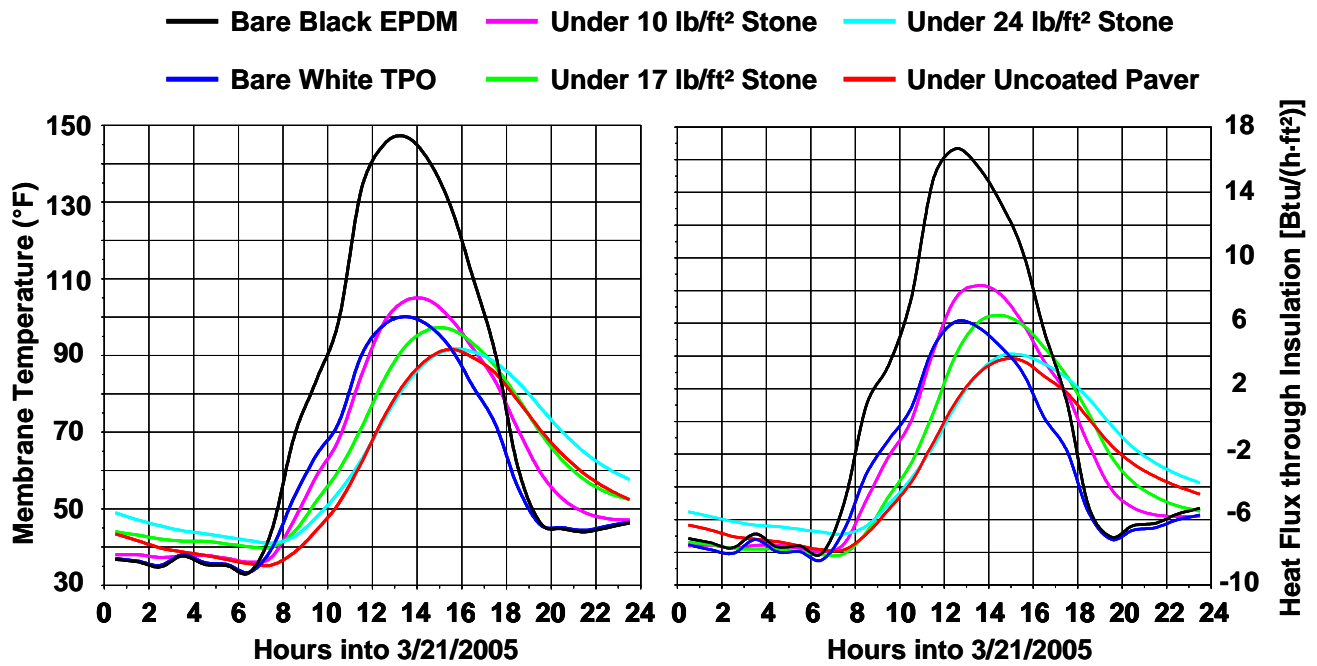
Figure 8. Membrane temperatures and roof heat fluxes twelve months into experimental program.
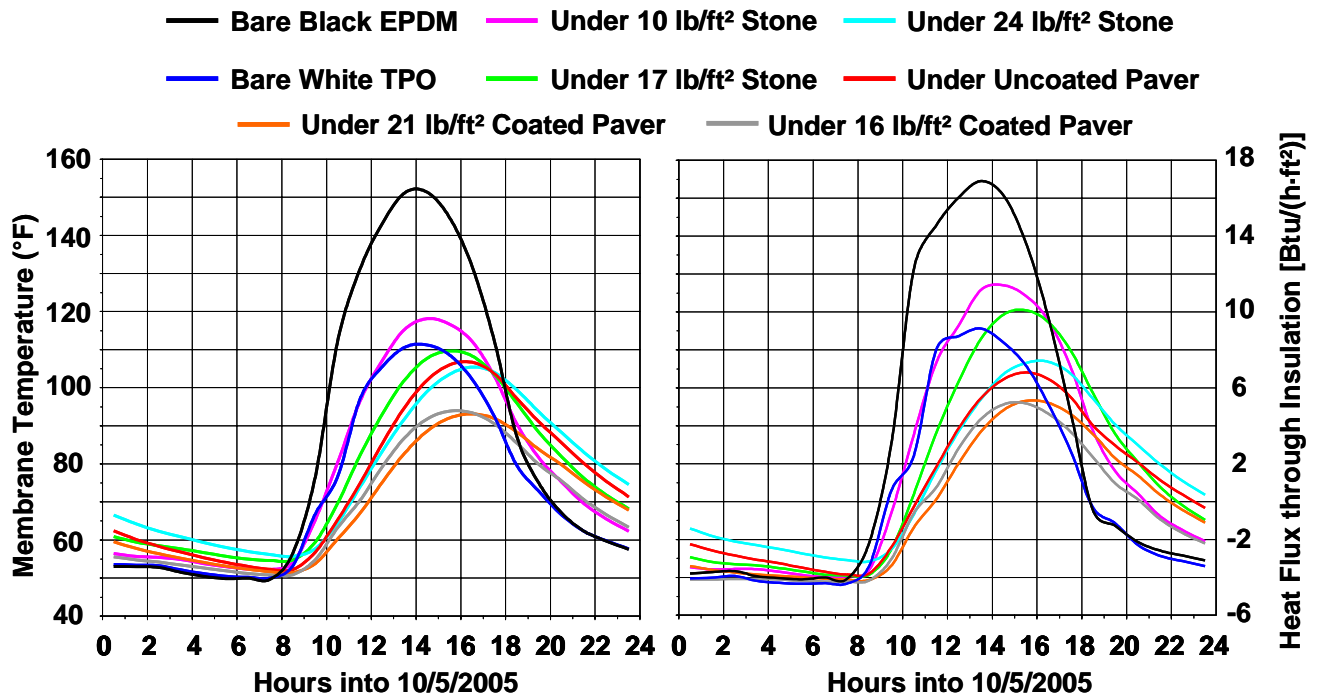

Figure 9. Membrane temperatures and roof heat fluxes nineteen months into experimental program.

Figures 9 through 12 include the membrane temperatures and roof heat fluxes for the coated pavers. The coated pavers combine the effects of high solar reflectance and high thermal mass. As expected, they perform better than any other system, showing the lowest peak membrane temperatures and heat fluxes.
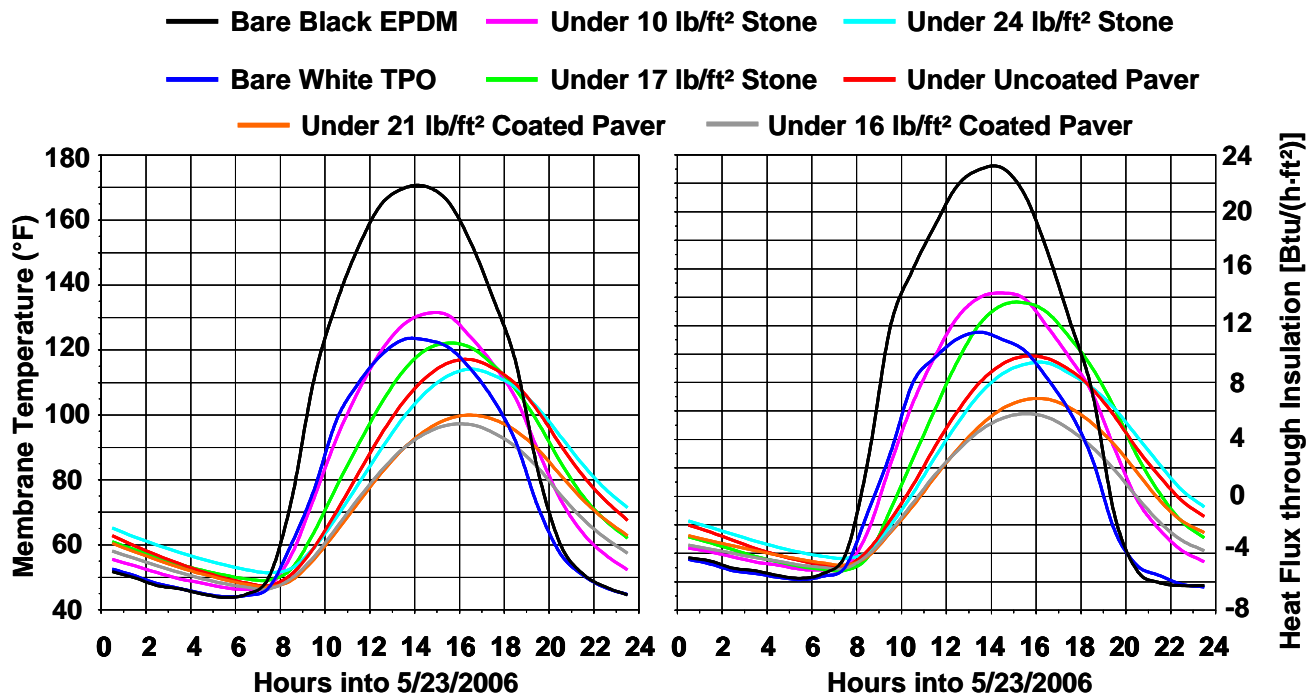

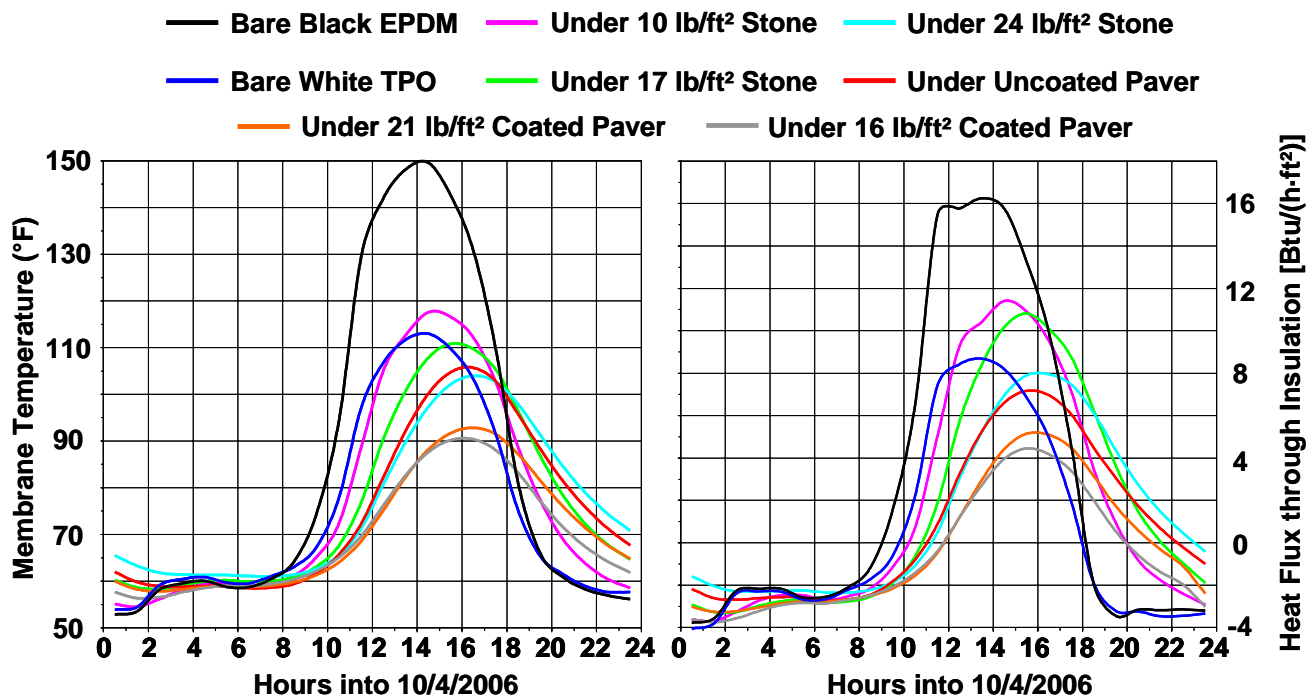**Figure 10.** Membrane temperatures and roof heat fluxes twenty-six months into experimental program.

Figure 11. Membrane temperatures and roof heat fluxes thirty-one months into experimental program.
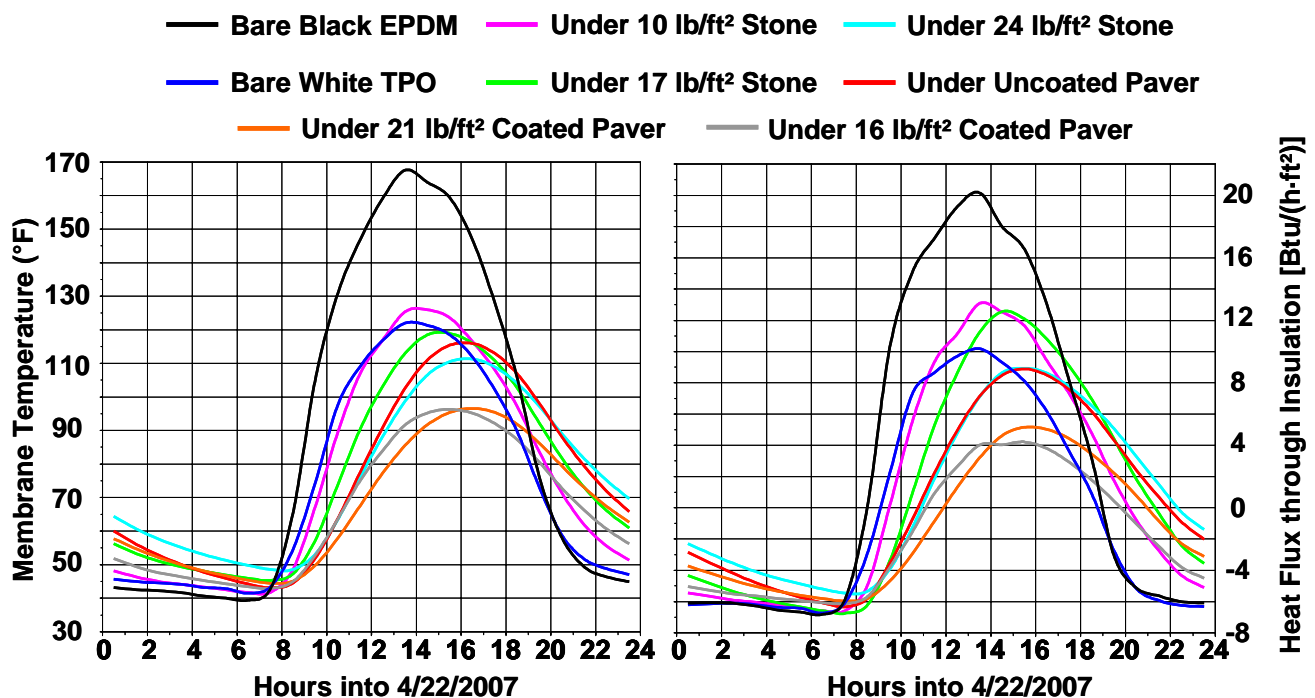
Figure 12. Membrane temperatures and roof heat fluxes thirty-seven months into experimental program.

The areal loading of the 21 lb/ft² coated paver is about the same as that of the 24 lb/ft² stone ballast and the uncoated paver so their peaks in membrane temperature and heat flux occur at about the same times. These times are slightly after those of the 16 lb/ft² coated paver and the 17 lb/ft² stone.

Measured Heat Fluxes, Cooling Loads and Heating Loads

The membrane temperatures presented in Figs. 6 through 12 were measured independently of the insulation heat fluxes. Therefore, they provide a useful check on the validity of the heat fluxes. After all, it is the temperature difference between the roof membrane and deck that drives heat through the roof. However, the heat fluxes are of primary interest as a measure of energy performance. Heat is what has to be removed in the form of cooling load or added in the form of heating load by the conditioning system in the building under the roof.

Figure 13 presents the average weekly heat fluxes at the location of the heat flux transducer in each system (see Fig. 3) over the course of the project. The three cooling seasons in the project are shown as the intervals from 4/20/2004 through 10/19/2004 (summer 2004), 4/21/2005 through 10/20/2005 (summer 2005), and 4/22/2006 through 10/21/2006 (summer 2006). The three heating seasons are 10/20/2004 through 4/20/2005 (winter 2004), 10/21/2005 through 4/21/2006 (winter 2005) and 10/22/2006 through 4/22/2007 (winter 2006).

The average weekly heat flux for the black system is generally the highest (largest positive number) for all systems each week during the summers. It is generally the smallest (smallest negative number) during the winters. The average weekly heat flux for the white system is the lowest during the first summer but not so in subsequent summers as it weathers and the coated pavers are brought on line. Complete weathering of the TPO membrane covering the white system is achieved by the start of the second summer. It is difficult to distinguish any difference among the average weekly heat fluxes for the
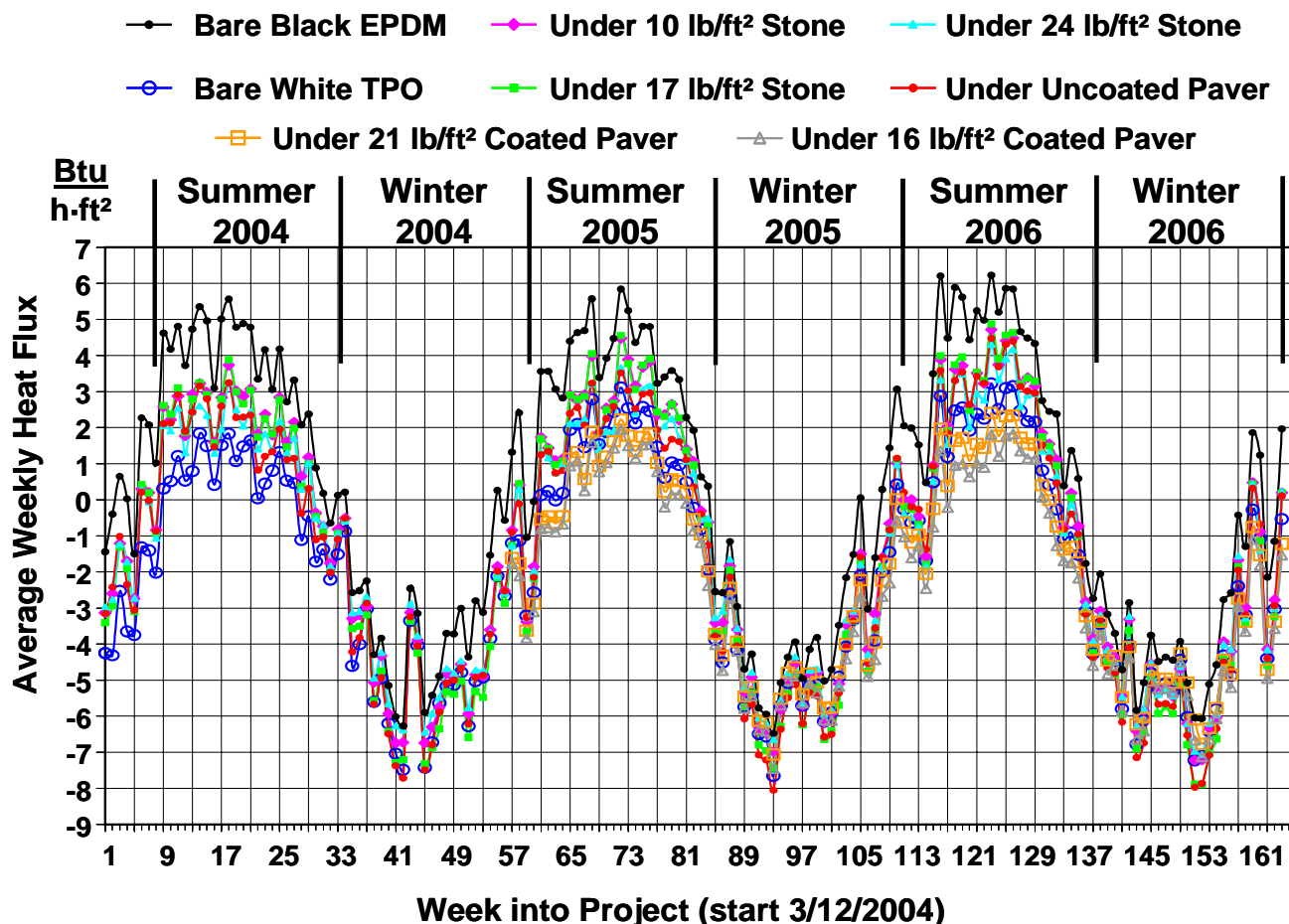
- 14 -

Figure 13. Average weekly heat fluxes for the ballasted and control systems over the three year duration of the project.

ballasted systems, except the coated pavers, during the summers. There is little difference among the average weekly heat fluxes for the ballasted systems and the white system during the winters.

The data from which Fig. 13 was prepared were further analyzed to generate comparisons of more relevance for energy performance of roof systems. With the sign convention implicit to Fig. 13, positive heat fluxes enter the building while negative heat fluxes leave the building through the roof. In the generation of average weekly heat fluxes, positive and negative heat fluxes can cancel. This can be misleading because building conditioning systems are either in cooling mode, in heating mode or off. In the DOE Cool Roof Calculator (Petrie *et al.,* 2001; Petrie *et al.,* 2004), cooling loads are defined as the annual sum of the positive heat fluxes through the roof deck when outside air temperature is greater than 75°F. Heating loads are defined as the sum of the negative heat fluxes through the roof deck when outside air temperature is less than 60°F. Not including the small heat fluxes between 75°F and 60°F is meant to approximate the dead band, at least that due to the roof, when the building under the roof needs neither heating nor cooling and the conditioning system is off.

These definitions were applied to the heat fluxes through the insulation for the three years. Using the insulation heat fluxes instead of deck heat fluxes was necessary because deck heat fluxes were not measured. Most of the annual cooling loads occurred during the summers defined in Fig. 13 and most of the annual heating loads occurred during the winters. This arbitrary division of each year into two

- 15 -

seasons was to generate smaller worksheets for organization and manipulation of the data. A summary worksheet combined the summer and winter results for each year.

Cooling and heating loads for the white system are shown in Table 2. Even for this relatively simple system, changes in climatic conditions from year to year and changes in the system itself make for complicated behavior. Changes in climatic conditions are represented by the 65°F heating and cooling degree-days calculated from the outdoor temperatures measured above the test sections. Loads for the white system are affected by the changes in solar reflectance of its TPO membrane, which were shown in Table 1. The decrease in solar reflectance due to weathering was complete by the start of the second year. This may explain part of the increase in cooling load from the first year to the second. The increase in heating load must be weather-related. Moreover, the loads for the second and third year would have been the same had climatic conditions not changed. Note that the changes in loads are at least qualitatively consistent with the changes in degree-days.

Table 2.
Measured cooling and heating loads for the white test section compared to
heating and cooling degree-days over the three years of the project

Year of Project	Cooling Load [Btu/·ft²]	Cooling Degree-Days [°F-day]	Heating Load [Btu/ft²]	Heating Degree-Days [°F-day]
2004	6960	1502	-22220	3614
2005	9340	1672	-23740	3947
2006	8790)	1560	-24740	4187

Figs. 13 applies only to the low R-value roofs for the climatic conditions in East Tennessee during the three years of the project. They provide experimental evidence that neither the cooling loads nor the heating loads are much different for conventional uncoated ballasted systems and the white system. This supports the conclusion of Desjarlais, *et al.* (2006) after two years that ballasted systems should be considered for "cool" status and the savings this implies. Possible operating cost savings depend not only on the heating and cooling loads, but also on the efficiency of the heating, ventilating and cooling equipment and the price of energy to run it. Equipment efficiency and energy prices should be the same for dealing with different roofs if they cause the same loads.

Properties Needed to Predict Energy Performance with STAR

To fulfill the goals of the project, an effort was made to model the behavior of the ballasted and control systems shown in Figure 13. Because of its use for the DOE Cool Roof Calculator and our extensive experience with it, the program STAR was chosen. It is a finite-difference form of the transient heat conduction equation in one dimension. All three types of boundary conditions are allowed at the inside and outside surfaces of a low-slope roof system. In the validation of the modeling for this project, the temperature measured at the top of the deck was used as the inside boundary condition. Data from the weather station on the test facility were used to impose convection and thermal radiation as the boundary condition at the outside of each system.

STAR also requires a layer by layer description of the physical and thermal properties of roof systems. The physical layout of the systems was shown in Fig. 3. Table 3 lists properties for initial runs of STAR. Data are listed for the three loadings of stone, the uncoated paver, the coated pavers, the exposed white and black membranes, and the two layers of wood fiberboard insulation that were used in each system.

Direct measurements were made of the thickness and density of the various components of the systems. The weight of several pavers of each type was measured by a scale and divided by the measured volume to yield density. A nominal 5-gallon bucket was weighed, filled with stone and weighed again. The actual volume of the bucket was determined by measuring the weight of water to fill it. Weight of stone divided by its volume yielded the average density of the stone including air spaces. The weight of water to fill the spaces around the stones yielded a porosity of 40%. Table 2 includes the ranges of solar reflectance for all surfaces that weathered, spanning the data presented in Table 1 for the smooth surfaces. Solar reflectance for the stone and the estimated infrared emittance for all surfaces are repeated from the discussion above of the test sections.

The thermal conductivity and specific heat of the white and black membranes and fiberboard were obtained from the literature and our own measurements. For the stone and pavers, the program Properties Oak Ridge (PROPOR) was used as part of the ongoing analysis of evolving data to estimate effective thermal conductivity and volumetric heat capacity (the product of density and specific heat). PROPOR compares temperatures and heat fluxes that are measured inside a system to those predicted by the transient heat conduction equation. Temperatures measured at the outside and inside surfaces are boundary conditions. Thermal conductivity and volumetric heat capacity are considered parameters. Values of the parameters are adjusted by an automated iteration procedure until best agreement is obtained. Best agreement is defined as the minimum of the squares of the differences between measured and predicted temperatures and heat fluxes inside the systems. An estimate of the confidence in the final parameter values is included as part of the output from the program (Beck *et al.,* 1991).

Use of PROPOR, which like STAR is based on a finite-difference form of the transient heat conduction equation, indicated that modeling the energy performance for the ballasted systems would be more difficult than for the black and white systems. PROPOR had difficulty converging to estimates of the thermal conductivity and volumetric heat capacity for the 10 lb/ft² and 17 lb/ft² loadings of stone except for several weeks during each winter in East Tennessee. Even then the estimates were not acceptably precise. Convergence for the 24 lb/ft² stone was less difficult. Convergence was obtained for the pavers no matter what the weather conditions.

Table 3.
Properties input to STAR for initial modeling of the ballasted and control systems

Component	Loading, lb/ft²	Thickness, in.	Thermal conductivity, Btu·in./(h·ft²·°F)	Density, lb/ft³	Specific heat, Btu/(lb·°F)	Infrared emittance, %	*Solar reflectance, %
10 lb/ft² stone	10.0	1.3	6.21 ±6	92.4	0.17 ±0.2	90	20
17 lb/ft² stone	16.9	2.2	5.94 ±7	92.4	0.21 ±0.3	90	20
24 lb/ft² stone	23.9	3.1	4.65 ±2	92.4	0.20 ±0.1	90	20
Uncoated paver	23.5	2.0	17.6 ±4	141	0.15 ±0.04	90	54 to 47
21 lb/ft² coated paver	21.4	1.69	6.13 ± 1	152	0.11 ± 0.03	90	73 to 71
16 lb/ft² coated paver	16.5	1.25	3.65 ± 0.7	158	0.083 ± 0.03	90	74 to 76
White membrane	negl.	0.050	1.2	58	0.4	90	70 to 60
Black membrane	negl.	0.045	1.2	58	0.4	90	8 to 9
Fiberboard	n.a.	0.5, 1.0	**a+b·T	17.5	0.19	not needed	not needed

* Ranges, if given, span observed variation over the three years of the project (see Table 1)
** From guarded hot plate measurements: $k_{fiberboard}$ [Btu·in./(h·ft²·°F)] = 0.3376 + 0.000746·T(°F)

One reason for the problems with convergence and lack of confidence is convection effects in loadings of stone during peak solar insolation. Another reason is inaccurate measurement of outside surface temperatures for all the ballasts. Unlike STAR, PROPOR requires temperatures at the surface as the only allowed type of boundary condition. For the ballasts, thermocouple measuring junctions were placed against two stones at the top of each stone loading (see Fig. 4) and slightly below the outside surface of the central paver for the uncoated and coated paver systems. Unreliable surface temperatures are more likely for the loadings of stone when the sun is high in the sky. Sunlight can penetrate as far as the black membrane and cause heating of the stones from below in addition to the usual heating from above.

The thermal conductivity and specific heat for the stone and paver systems in Table 3 are the averages of estimates from PROPOR for weeks when it converged. The uncertainty reported by PROPOR is appended to these estimates. Specific heat is obtained by dividing the estimated volumetric heat capacity by the measured density. Only the volumetric heat capacity is used by PROPOR and STAR. The uncertainties in the estimates for both properties of the stone are of the order of 50% to 150% of the estimates themselves. Furthermore, effective thermal conductivity and, to a lesser extent, specific heat vary with stone loading. This would not be true if heat transfer through the stone were strictly a heat conduction phenomenon, or at least apparent thermal conduction, like conduction and radiation in mass insulation. The three loadings were obtained with the same stone; only the thickness was changed.

The 0.19 to 0.24 Btu/(lb·°F) range for specific heat of heavyweight concrete (ASHRAE 2005) and the specific heat of 0.24 Btu/(lb·°F) for air compare well to values for the ballast in Table 3. ASHRAE

handbook values of the thermal conductivity of heavyweight concrete are given as the range from 9.0 to 18.0 Btu·in./(h·ft²·°F), which includes the values for the uncoated paver but not the coated pavers in Table 3. Possible values for the thermal conductivity of the stone are given by Côté and Konrad (2005). The porosity of the stone was measured as 40%. Côté and Konrad's data for granite and limestone show a thermal conductivity of 1.80 Btu·in./(h·ft²·°F) at this porosity, 29 to 39% of the values for the stone ballasts in Table 3.

An attempt was made to measure the thermal conductivity at 75°F of the stone and pavers by ASTM C518-98: Standard Test Method for Steady-State Heat Flux Measurements and Thermal Transmission Properties by Means of the Heat Flow Meter Apparatus (ASTM, 1998). Samples of the stone and uncoated paver were sandwiched between pieces of foam to protect the apparatus and provide the required level of thermal resistance. The foam used was characterized separately. Differences between R-values and thicknesses with and without the stone yielded stone sample thermal conductivity of 1.86 Btu·in./(h·ft²·°F) for heat flow up and 1.76 Btu·in./(h·ft²·°F) for heat flow down. The average 1.81 Btu·in./(h·ft²·°F) agrees with the data from Côté and Konrad. Slightly higher thermal conductivity for heat flow up is consistent with the effect of air between the individual stones. By the same technique, the uncoated paver had thermal conductivity of 6.58 Btu·in./(h·ft²·°F), 27% of the value in Table 3.

Diurnal Behavior of Measurements and of Predictions Using Initial Estimates of Properties

STAR was executed with the properties in Tables 1 and 3, yielding hourly predictions of membrane temperatures and insulation heat fluxes for all three years of the project. The thermal conductivity and specific heat in Table 3 for the ballasts were considered initial values. Because of the large uncertainty of their estimation by PROPOR and the low values of thermal conductivity indicated by the literature and the C518 measurements, it was unlikely that they would yield acceptable agreement with measurements. A trial-and-error process was anticipated to select final values. Modeling the behavior of the exposed white and black membrane systems was straightforward.

The predicted membrane temperatures and insulation heat fluxes were entered in a spreadsheet that contained the hourly averages of the measurements. Graphs were generated for selected days to show diurnal behavior and indicate agreement between measurements and predictions. Clear days show maximum solar effect and have smooth curves through the hourly temperatures and heat fluxes. There are few deviations caused by cloudiness and inclement weather that make it difficult to visually compare the data. Figure 14 shows a typical clear day during the second summer of the project, by which time the solar reflectance of the white surface had decreased to 62%.
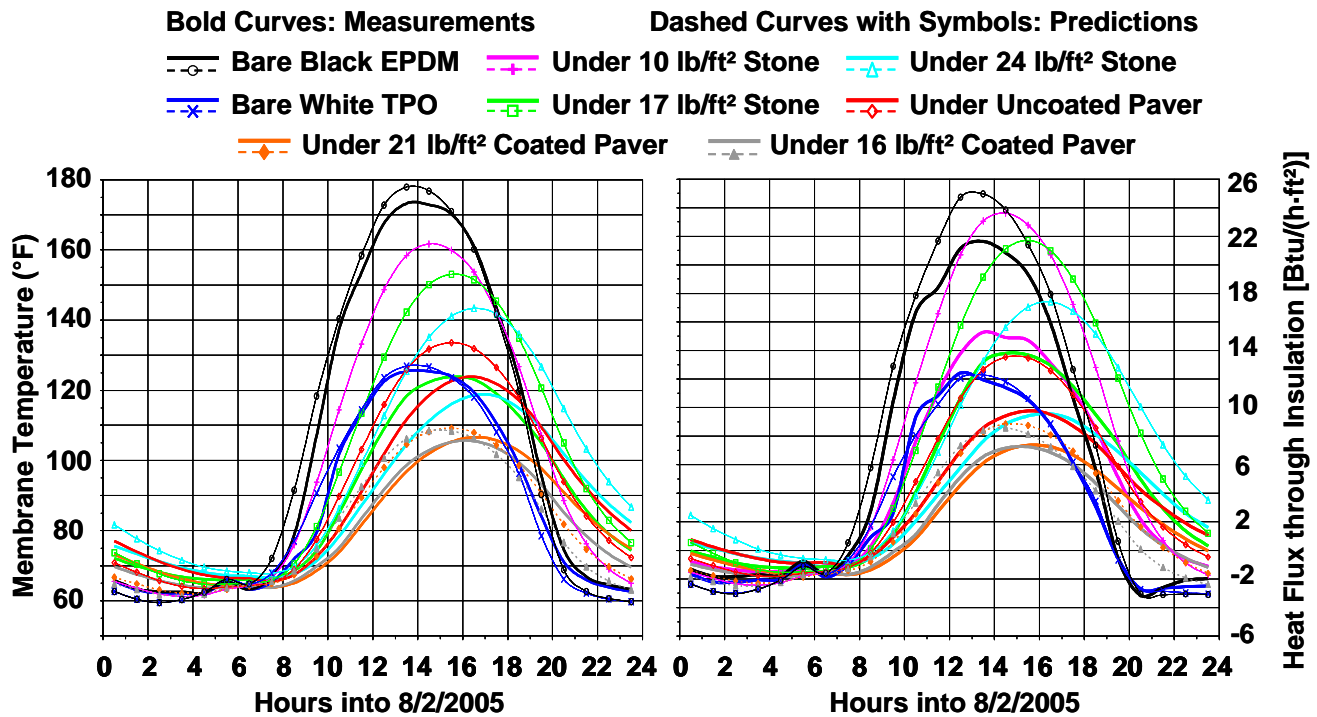
Figure 14. Diurnal behavior of measurements and predictions using properties in Tables 1 and 3 for a typical clear day during Summer 2005.

The black and white systems are lightweight systems with R-3.8 fiberboard insulation. The ballasted systems are thermally massive with the same insulation. Thicknesses from Table 3 and our measurements of apparent thermal conductivity with ASTM C 518 yield additional R-value of 0.7, 1.2 and 1.7 for the 10 lb/ft², 17 lb/ft² and 24 lb/ft² stone-ballasts, respectively. The uncoated paver, 21 lb/ft² coated paver and 16 lb/ft² coated paver add R-value of 0.3, 0.3 and 0.2, respectively. Figure 14 shows that peak values of the measured membrane temperature and insulation heat flux and the times when peaks occur are affected by the thermal mass and, possibly, extra R-value of the ballasts.

The time at which peak heat flux occurs is important to operation of the building under a low-slope roof system. Measurements for the ballasted systems show consistent delays relative to the black and white systems. For ten clear days over the course of the project, comprising the days selected for Figs. 6 through 12 and, later, Figs. 15, 16 (same day as Fig. 14) and 17, the average times of peak heat flux for the white and black systems coincide within 0.2 h. Relative to the black system, the 10 lb/ft², 17 lb/ft² and 24 lb/ft² stone-ballasts show delays of 1.0 h, 1.8 h and 2.7 h, respectively. The uncoated paver, 21 lb/ft² coated paver and 16 lb/ft² coated paver show delays of 2.3 h, 2.6 h and 1.8 h, respectively. This variation generally agrees with the variation of the loading of the respective systems in Table 3. The delays are clearly not consistent with added R-value because the pavers show delays like the medium and heavy stone loadings. This proves that the ballasted systems show significant and consistent effect of their thermal mass.

The relatively simple behavior of exposed white and black membranes over a low-slope roof with low thermal mass is well understood from previous experience with test sections used to validate STAR for the DOE Cool Roof Calculator (Petrie, 2001). On the clear days the hourly predictions for the exposed white membrane were in good agreement with the measurements and consistent with our understanding.

The hourly behavior of the exposed black membrane, when compared to that from previous experience, indicates that the measured temperatures are accurate but the measured heat fluxes are low. Temperatures and heat fluxes were measured independently with thermocouples and small heat flux transducers, respectively. More uncertainty in measured heat fluxes is consistent with our experience. It occurs despite calibration of the heat flux transducers in the wood fiberboard insulation according to ASTM C 518.

As a specific example of the greater uncertainty in measured heat fluxes, the coated pavers were removed in Summer 2007 in preparation for a new experiment on the RTRA. This exposed the black EPDM membranes under them. After cleaning the membranes, additional data were obtained from these systems and the exposed black membrane that served as a control during the ballast project. The relatively steady heat fluxes through the three test sections were compared in mid to late afternoon during a week without rain.

Relative to the average from the three heat flux transducers [of the order of 20 Btu/(h·ft²)], heat flux under the black control was 4.9% low, heat flux for the black membrane that was under one paver was 2.6% low and heat flux for the black membrane that was under the other paver was 7.5% high. From this and other experience, we consider heat fluxes to be uncertain from ±5% to ±10%. During the same time and relative to the average temperature from the thermocouples under the three membranes [of the order of 160°F], the membrane temperatures were 1.0% high, 3.0% low and 2.1% high for the same systems. Assuming identical thermocouples, this indicates that variability in the configuration of the test sections causes uncertainty. Again, from this and other experience, we consider it to be from ±2% to ±3%.

The shape of the predicted curves on the clear days is correct for the control systems, with low thermal mass and either an exposed white or black membrane. Predicted peak times coincide with the measured peak times. The nighttime predictions are generally low for both these controls. This is likely due to the effects of condensation and no attempt was made to model its effect.

Little positive can be said about the predictions of membrane temperature and insulation heat flux for the ballasted systems with properties in Table 3. Peak times generally coincide with measured peak times. Agreement in early morning between predictions and measurements is acceptable for the light and medium loadings of stone, but not for the heavy stone loading or any of the pavers. However, predicted peak values for all ballasted systems are significantly higher than the corresponding peak measurements. This is the dominant feature of Fig. 14 and precludes having any confidence in the accuracy of the predictions, night or day, using the set of properties in Table 3.

Diurnal Behavior of Measurements and of Predictions Using Final Estimates of Properties

Trials for the ballasted systems indicated that peak times are most sensitive to specific heat. If specific heat is increased, peak time is delayed. Peak values are most sensitive to thermal conductivity. If thermal conductivity is decreased, the peak membrane temperature and insulation heat flux also decrease. However, to some extent, changes in specific heat affect peak values and changes in thermal conductivity affect peak times. STAR was executed with thermal conductivity values for the stone and paver systems that were varied as a percentage of the values in Table 3. Specific heat was varied less, seeking a common value for the stone and another for the pavers.

The best overall agreement between predictions and measurements was judged to occur for thermal conductivity corresponding to 10%, 15% and 20% of Table 3 values for the 10 lb/ft², 17 lb/ft² and 24

lb/ft² stone-ballasted systems, respectively, and 20%, 80% and 80% for the uncoated paver, 21 lb/ft² coated paver and 16 lb/ft² coated paver systems, respectively. These values are 34% to 74% of the values measured by ASTM C518.

The specific heat for the stone was chosen to be 0.10 Btu/(lb$_m$·°F). For the pavers 0.21 Btu/(lb$_m$·°F) was chosen. The ASHRAE Handbook of Fundamentals (ASHRAE 2005) lists 0.19 to 0.24 Btu/(lb$_m$·°F) as the range for heavyweight concretes, yielding a geometric mean of 0.21 Btu/(lb$_m$·°F). Table 4 lists the complete set of property values, repeating unchanged values from Table 3. Table 1 continues to apply for the seasonal variation of solar reflectance of the smooth surfaces.

Table 4.
Properties input to STAR for final modeling of the ballasted and control systems

Component	Loading, lb/ft²	Thick-ness, in.	Thermal conductivity, Btu·in./(h·ft²·°F)	Density, lb/ft^3	Specific heat, Btu/(lb·°F)	Infrared emittance, %	*Solar reflectance, %
10 lb/ft² stone	10.0	1.3	0.621	92.4	0.10	90	20
17 lb/ft² stone	16.9	2.2	0.891	92.4	0.10	90	20
24 lb/ft² stone	23.9	3.1	0.930	92.4	0.10	90	20
Uncoated paver	23.5	2.0	3.52	141	0.21	90	54 to 47
21 lb/ft² coated paver	21.4	1.69	4.90	152	0.21	90	73 to 71
16 lb/ft² coated paver	16.5	1.25	2.92	158	0.21	90	74 to 76
White membrane	negl.	0.050	1.2	58	0.4	90	70 to 60
Black membrane	negl.	0.045	1.2	58	0.4	90	8 to 9
Fiberboard	n.a.	0.5, 1.0	**a+b·T	17.5	0.19	not needed	not needed

* Ranges, if given, span observed variation over the three years of the project (see Table 1)
** From guarded hot plate measurements: $k_{fiberboard}$ [Btu·in./(h·ft²·°F)] = 0.3376 + 0.000746·T(°F)

Figures 15, 16 and 17, for clear days during the three summers of the project, show the much improved agreement between predictions and measurements for the ballasted systems when the properties in Table 1 and 4 are used. Predictions for the controls are unchanged. Note that the predictions for the white system, which incorporate the changing solar reflectance of this system, agree with the measurements. Peaks for it increase in the second summer day (Fig. 16) relative to the first summer day (Fig. 15) but are about the same in the second and third summer days (Figs. 16 and 17). Predicted peak temperatures and heat fluxes for all ballasts agree very well with measurements. Predicted peak times for the stone ballasts do not coincide exactly with the observed peak times, because the same specific heat was imposed for all three stone ballasts. The same specific heat for all pavers works well since all are made from concrete.

Generally, for all days and all systems, there are anomalies in the measurements that a model like STAR, with relatively few parameters, cannot duplicate. The comparatively low measured heat fluxes for the black control were mentioned above. The predictions for it are considered more accurate. Other anomalies were associated with moisture effects that STAR did not model. Dew or frost persisted on the exposed membranes well into mid-morning of many days. The 10 lb/ft² and 17 lb/ft² stone-ballasted
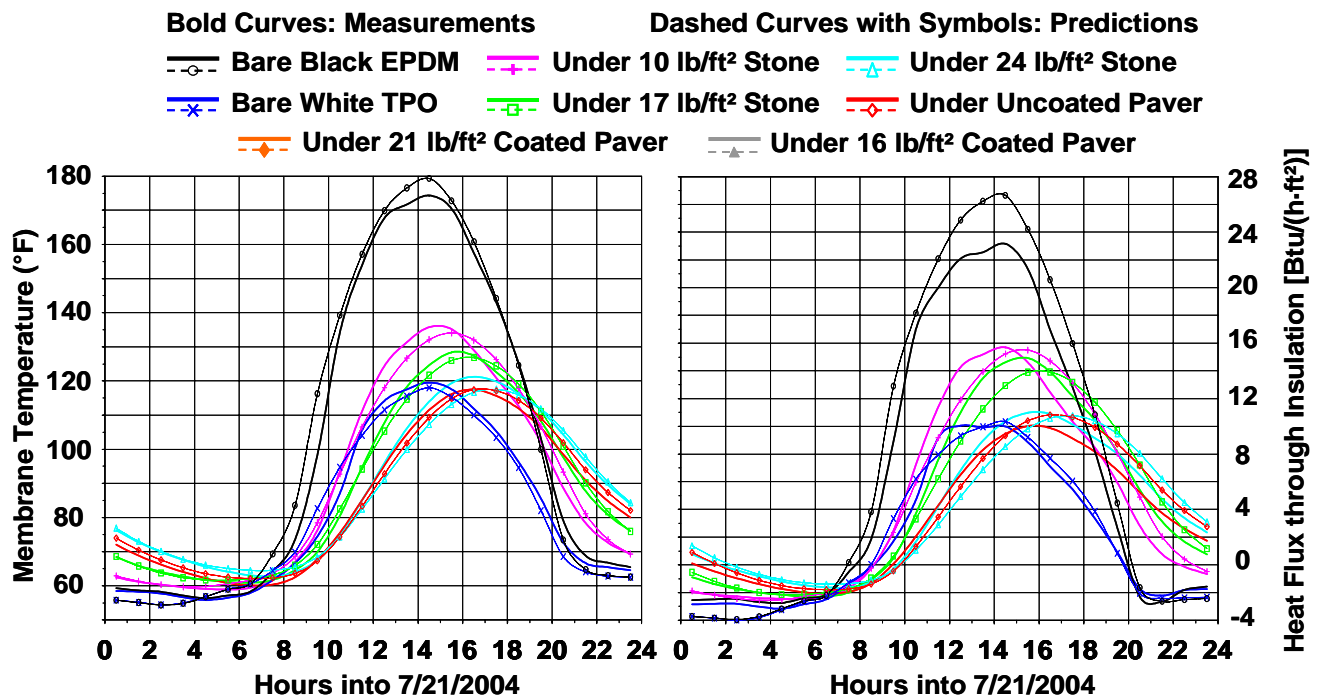
Figure 15. Diurnal behavior of measurements and predictions using properties in Tables 1 and 4 for a typical clear day during Summer 2004.
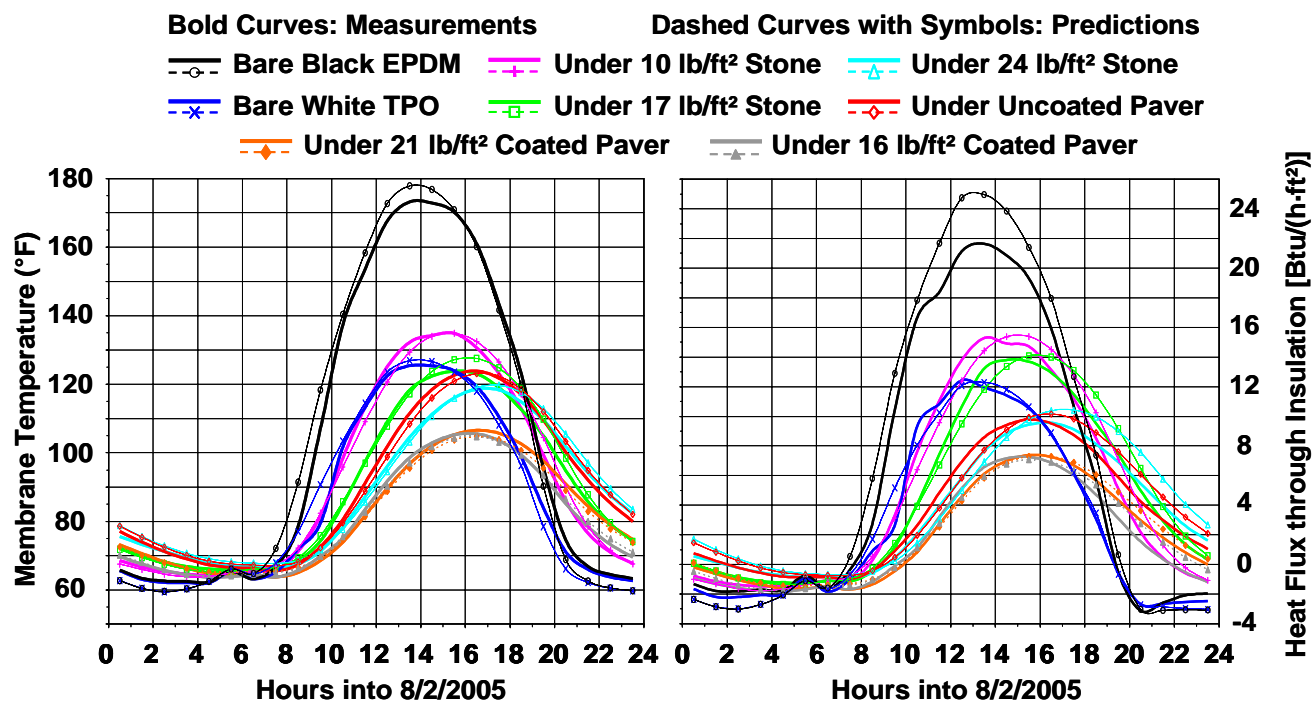
Figure 16. Diurnal behavior of measurements and predictions using properties in Tables 1 and 4 for a typical clear day during Summer 2005.
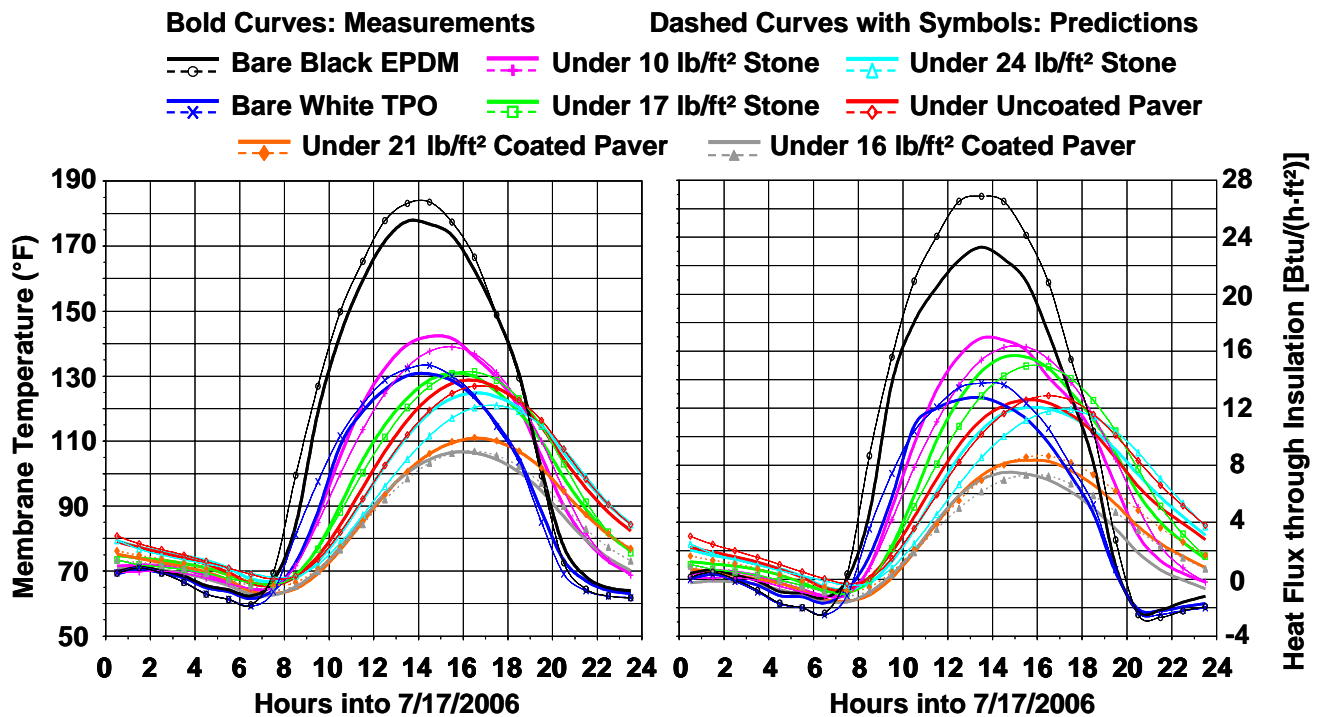
Figure 17. Diurnal behavior of measurements and predictions using properties in Tables 1 and 4 for a typical clear day during Summer 2006.

systems shared a test section, with the 10 lb/ft² system on the lower end of the low-slope roof of the test building. Rain on it and on the 17 lb/ft² test section drained through it and took a day or more after rain events. Rain on the 24 lb/ft² stone-ballasted test section, even though it occupied the high end of its test section, took several days to drain because the uncoated pavers were downstream of it. Rain drained quickly from the white control on the high end of the roof but did pond on its downstream partner, the black control. Rain did not seem to affect the coated pavers because it did not penetrate either system.

Comparison of Cooling and Heating Loads from Predictions and Measurements

As explained above, final estimates were made by trial-and-error of the effective thermal conductivity and specific heat needed to model the diurnal behavior of the ballasted systems with the transient heat conduction equation. Emphasis was on summer behavior because the primary goal of the project was to compare energy performance of ballasted systems and white systems. Furthermore, there were few sunny days during the winter seasons when the measured behavior did not show anomalies. To test the usefulness of the final estimates of ballast properties for STAR, cooling and heating loads were generated using data in Tables 1 and 4. The resulting differences between predicted cooling loads for the proposed systems and predicted cooling loads for the white system are added to produce Fig. 18. The resulting differences between predicted heating loads for the white system and predicted heating loads for the proposed systems are added to produce Fig. 19.

Figure 18 confirms that the good agreement between predictions and measurements, seen in Figs. 15 through 17, carries through to the cooling loads. The predicted and measured differences for the black system are in worse agreement than is the case for any ballasted system. This is attributed to the consistently low measured heat flux for the black control. For all systems, the variation from year to year
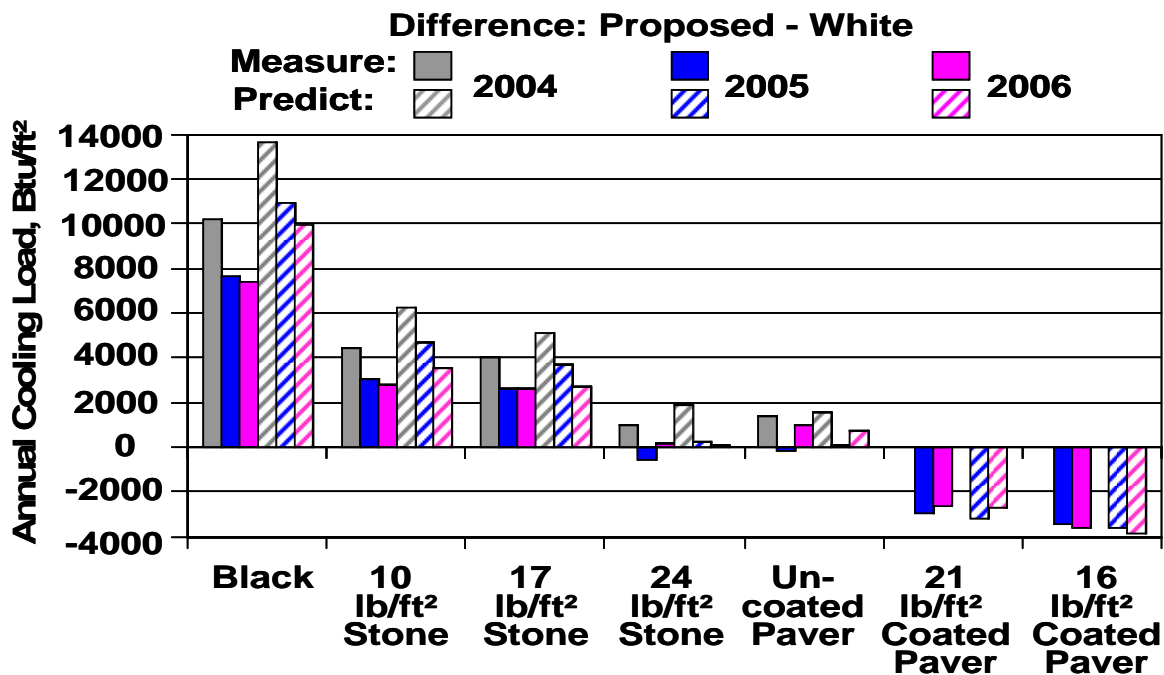
Figure 18. Differences in cooling loads between the proposed and white systems during the years of the project. Predictions use properties in Tables 1 and 4.

in the predicted differences in cooling loads follows the measured differences remarkably well. Both the effect of solar reflectance and the effect of thermal mass are captured by STAR, especially for the coated pavers. For the stone ballasts, the use of an effective thermal conductivity that decreases with increased loading, as shown in Table 4, accounts for the solar effects during cooling seasons. The differences between cooling loads for the ballasted systems and the white system are small, but are predicted accurately as a function of ballast loading and ballast type. The predictions for the light and medium loading of stone are more conservative than the measurements. The predictions for the heavy loading of stone and the uncoated paver confirm that they have the same cooling load as the white system.

As Fig. 19 shows, the properties of ballasts that do well for cooling loads do not work for heating loads. Only the predictions for the coated pavers are reasonable. For the other ballasted systems, predicted heating loads are significantly smaller than measured. That is, the predicted differences in heating loads between the proposed and white systems using properties in Table 4 are significantly larger than the measured differences. A 92% reduction on average would yield exact agreement with the measured differences. A reduction of only 58% on average results if the thermal conductivities in Table 3 are used along with a specific heat of 0.10 Btu/(lb$_m$·°F) for these ballasts. Reduction of the specific heat to 0.01 Btu/(lb$_m$·°F) decreases the differences another 11%, but is physically impossible. Thermal conduction alone is too simple a mechanism to use to predict the heating load of the ballasted systems.

The saving fact remains that the measured differences in heating load between the white system and the ballasted systems are small and random. The rain water retention on the 24 lb/ft² stone-ballasted system makes it behave more like the 21 lb/ft² coated paver than the uncoated paver in Fig. 19. It behaved like the uncoated paver on the clear days shown in Figs. 6 through 12. Predicted heating loads for the
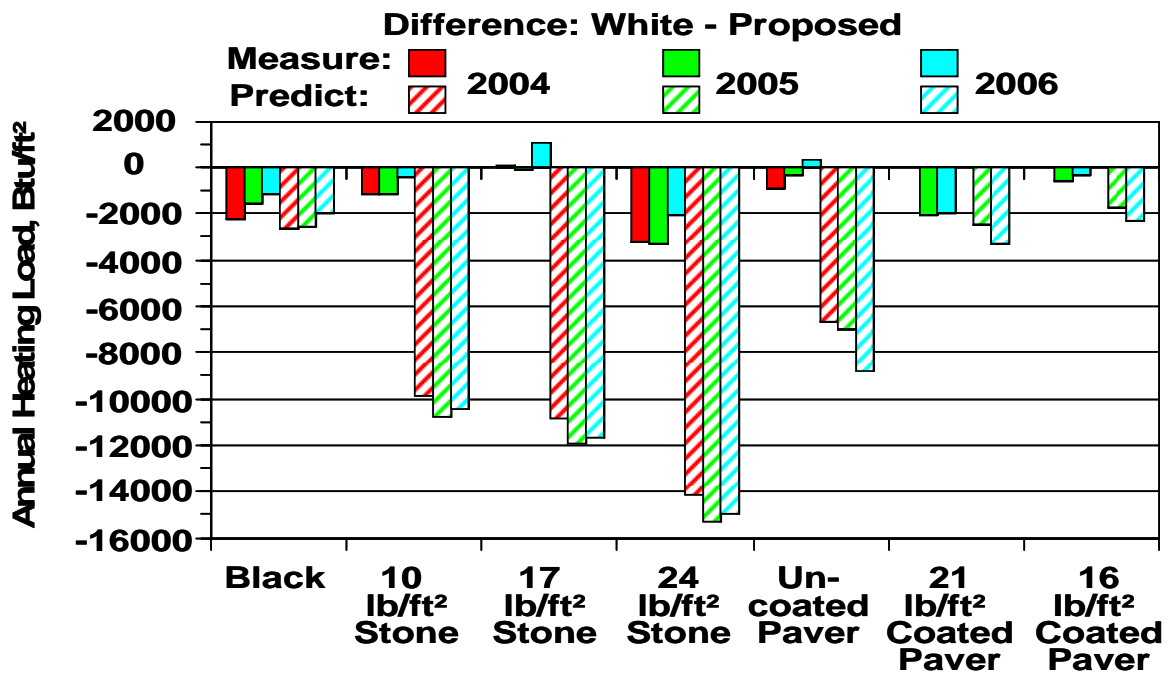
Figure 19. Differences in heating loads between the white and proposed systems during the years of the project. Predictions use properties in Tables 1 and 4.

weathered white system can serve for the heating loads of the conventional ballasted systems. Heating loads for the coated pavers are of little interest.

Cooling Loads for Varying Insulation and Location

The test sections for the project were insulated with only R-3.8 of fiberboard to maximize the sensitivity of the measurements to differences among the test sections. This is not the typical amount of insulation so the procedures used to develop the DOE Cool Roof Calculator (Petrie, *et al.* 2001) were applied to the ballasted systems. The coated pavers were not included because they are of limited commercial interest. STAR was run for climates from Anchorage to Phoenix. Ballast properties in Table 4 were used and roof insulation level was varied from R-5 to R-32. Cooling loads through the deck were generated from the hourly output. They were fit as a function of location-dependent cooling index and R-value for each system. Fits from the calculator were used for two white systems. The best white system has solar reflectance of 70%. The worst white system has solar reflectance of 48%, observed for weathered coatings (Petrie, *et al.*, 2001). The weathered solar reflectance for the white TPO membrane in this project is 60%.

Figure 20 compares annual cooling loads for three different locations and three different levels of insulation in the roofs. The test situation is approximately R-4 roof insulation in Oak Ridge Year 1. R-11 and R-19 are required by California Title 24 for nonresidential buildings. As expected the cooling loads decrease almost linearly with increasing insulation R-value at each location. California climate zone 12 (CZ12) has 12% fewer cooling degree-days and 36% more average solar insolation than Oak Ridge. This results in slightly larger cooling loads than in Oak Ridge. California climate zone 15 (CZ15) has 194% more cooling degree-days and 46% more average solar insolation than Oak Ridge. This desert climate causes very much larger cooling loads than in Oak Ridge. For any R-value and location, the cooling loads for the ballasted systems, except the 10 lb/ft² system, are between those for the best and worst white systems. In year 1 the white control system in this project had the solar reflectance of the

best white system. For years 2 and 3 its weathered solar reflectance was halfway between that of the best and worst white systems. The heavy loading of stone and the uncoated paver have about the same cooling load as such a system regardless of location or level of roof insulation.
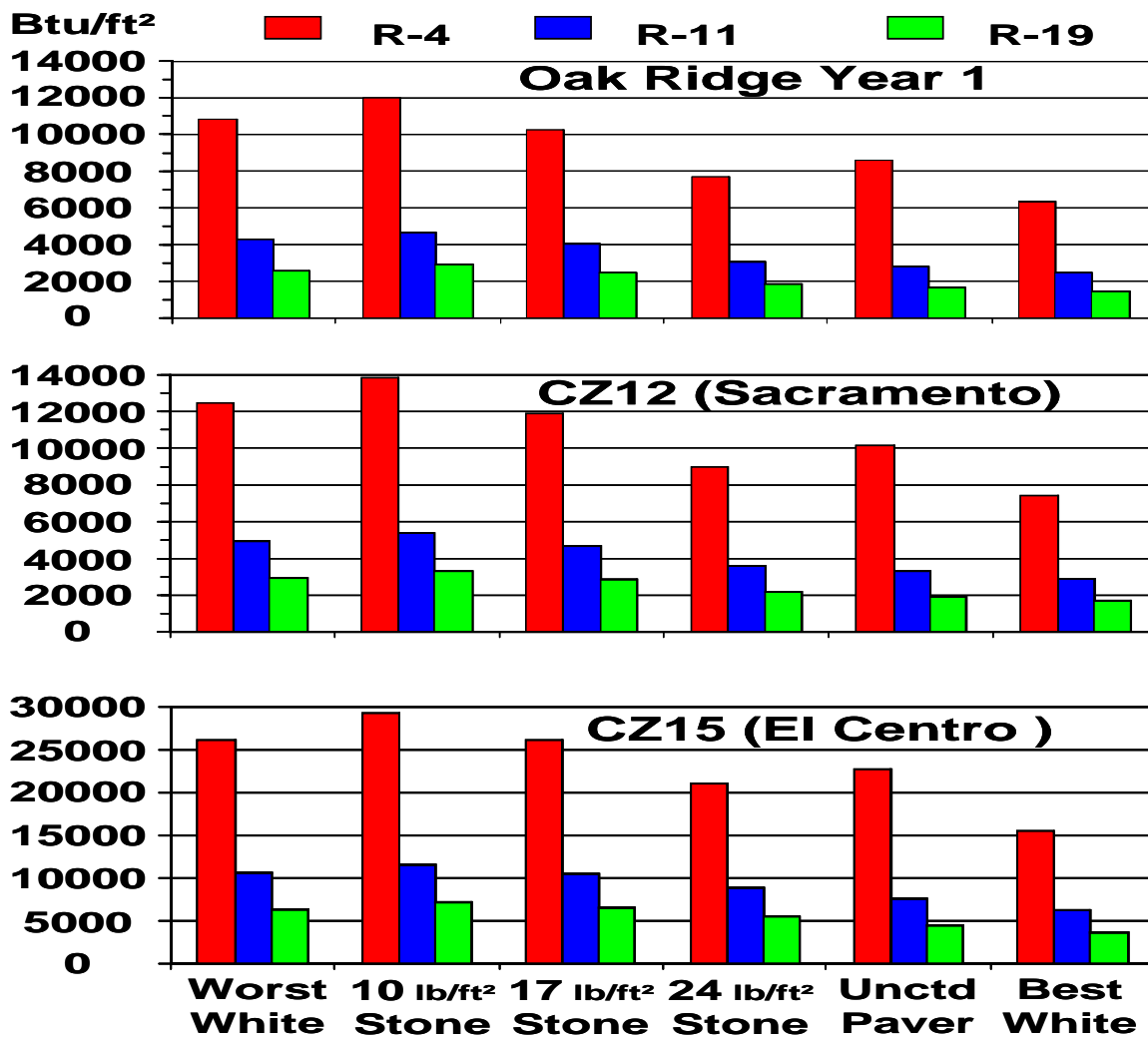

Figure 20. Predicted cooling loads as a function of roof insulation level in Oak Ridge Year 1, California Climate Zone 12 (Sacramento) and Climate Zone 15 (El Centro).

Conclusions

Three full years of continuous monitoring in the mixed climate of East Tennessee yielded data to compare the energy performance of six ballasted systems and a system with an exposed black membrane to that of a system with an exposed white membrane. Heat fluxes through the insulation in each test section were used to obtain the annual cooling and heating loads due to unit area of each system. The following conclusions can be drawn:

- The cooling loads for the heavy and medium stone-ballasted and uncoated paver-ballasted systems were approximately the same as for the white system.
- Cooling loads for the light weight stone systems were slightly larger than for the white system but significantly less than for the black system.

- Cooling loads for coated pavers with heavy and medium loading showed cooling loads significantly less than for the white system.
- Only the cooling load of the white system showed significant effects of weathering, which was complete by the start of the second year of the project.
- Heating loads for the ballasted systems showed random variation as loading increased and type changed. Except for the heavy weight stone system, they were about the same as for the white system.
- The heavy weight stone system showed slightly less heating load than the black system but this is considered an anomaly due to rain effects.
- All evidence on clear days of diurnal behavior showed the heavy weight stone and uncoated paver systems performing equally due to the same thermal mass despite different solar reflectance.

An effort was made to model heat flow through the ballasted systems with transient heat conduction alone, using the program STAR. STAR has successfully modeled non-ballasted systems in past projects and did so again in this project. Trial-and-error was required to duplicate diurnal variation of measured membrane temperatures and insulation heat fluxes on clear days for the ballasts. Effective thermal conductivities 34% to 74% of measured values resulted for the stone and paver systems. Specific heats were close to literature values. With these properties:

- The predicted cooling loads showed the same variation with ballast loading and type as the measurements.
- Predictions of cooling loads were made using the procedures of the DOE Cool Roof Calculator for higher levels of roof insulation and more severe cooling climates than for the measurements.
- Ballasted systems performed relative to white systems like they did in the measurements.
- Contrary to the measurements, these properties predicted heating loads for the conventional ballasts much smaller than heating loads for the white system.
- Heating loads for the coated pavers were predicted well but coated pavers are not commercially available systems. High effective thermal conductivities and unrealistically low specific heats still did not yield heating loads like the measurements. It is concluded that transient heat conduction alone is not adequate to predict heating loads for ballasts.

References

ANSI, 2001. ANSI/SPRI RP-4, "Wind Design Standard for Ballasted Single-Ply Roofing Systems" ANSI. New York, NY.

ASHRAE. 2005. "2005 ASHRAE Handbook: Fundamentals," Chapter 25, Table 4; Chapter 39, Table 3. Atlanta: American Society of Heating, Refrigerating and Air Conditioning Engineers, Inc.

ASTM, 1997. ASTM E 1918-97, Standard Test Method for "Measuring Solar Reflectance of Horizontal and Low-Sloped Surfaces in the Field." ASTM International, Philadelphia PA.

ASTM, 1998. ASTM C 518-98, Standard Test Method for "Steady-State Heat Flux Measurements and Thermal Transmission Properties by Means of the Heat Flow Meter Apparatus." ASTM International, Philadelphia PA.

ASTM, 2004. ASTM C 1549-04, Standard Test Method for Determination of Solar Reflectance Near Ambient Temperature Using a Portable Solar Reflectometer." ASTM International, Philadelphia PA.

Beck, J.V., Petrie, T.W. and Courville, G.E., 1991. "Using Parameter Estimation to Analyze Building Envelope Thermal Performance," pp. 161-191, Special Report 91-3. *In-Situ Heat Flux Measurements in Buildings: Applications and Interpretations of Results*. S.N. Flanders, Editor. Hanover, NH: U.S. Army Cold Regions Research and Engineering Laboratory.

Côté, J. and Konrad, J-M., 2005. "Thermal Conductivity for Base-Course Materials," pp. 61-78, *Canadian Geotechnical Journal,* vol. 42, no. 11.

Desjarlais, A., Petrie, T., Miller, W., Gillenwater, R., and Roodvoets, D., 2006 "Evaluating the Energy Performance of Ballasted Roof Systems," presented at and published in the proceedings of 3rd International Building Physics Conference, Montreal, August 27-31, 2006.

Gillenwater, Dick, Petrie, Tom, Miller, Bill, and Desjarlais, Andre, 2005. "Are Ballasted Roof Systems Cool?" presented at Roof Consultants Institute May 2005 Conference "Cutting Through the Glare" and published in pp. 32-44, *RCI Interface*, vol. XXIII, no. 9 (September 2005).

Miller, W.A., Cheng, M.D., Pfiffner, A., and Byars, N., 2002. "The Field Performance of High-Reflectance Single-Ply Membranes Exposed to Three Years of Weathering in Various U.S. Climates." ORNL/TM-2002. Oak Ridge, TN, Oak Ridge National Laboratory.

Miller, W.A. and Roodvoets, D., 2004. "Saving Energy by Cleaning Reflective Thermoplastic Low-Slope Roofs," in proceedings of *Performance of Exterior Envelopes of Whole Buildings IX.* Atlanta: American Society of Heating, Refrigerating and Air Conditioning Engineers, Inc.

Miller, W.A., Roodvoets, D.L. and Desjarlais, A., 2004. "Long Term Reflective Performance of Roof Membranes," in proceedings of the 2004 Roof Consultants Institute Convention.

Petrie, T.W., Desjarlais, A.O., Robertson, R.H., and Parker, D.S., 2000. Comparison of techniques for in-situ, non-damaging measurement of solar reflectance of low-slope roof membranes. ,14th Symposium on Thermophysical Properties, International Journal of Thermophysics, Boulder, CO: National Institute of Standards and Technology.

Petrie, T.W., Atchley, J.A., Childs, P.W. and Desjarlais, A.O., 2001. "Effect of Solar Radiation Control on Energy Costs – A Radiation Control Fact Sheet for Low-Slope Roofs," in proceedings of *Performance of the Exterior Envelopes of Whole Buildings VIII: Integration of Building Envelopes*. Atlanta: American Society of Heating, Refrigerating and Air-Conditioning Engineers, Inc.

Petrie, T.W., Wilkes, K.E. and Desjarlais, A.O., 2004. "Effect of Solar Radiation Control on Electricity Demand Costs–an Addition to the DOE Cool Roof Calculator," in proceedings of *Performance of Exterior Envelopes of Whole Buildings IX*. Atlanta: American Society of Heating, Refrigerating and Air Conditioning Engineers, Inc.

Wilkes, K.E., 1989. Model for Roof Thermal Performance. ORNL/CON-274. Oak Ridge, TN, Oak Ridge National Laboratory.